Supporting Information

3D-printed Ultra-high Se loading Cathode Enabled Continuous Li^+ Immigration for High Energy Density Quasi-Solid-State Li-Se Batteries

Xuejie Gao,[a, b, #] Xiaofei Yang,[a, #] Sizhe Wang,[a] Qian Sun,[a] Changtai Zhao,[a] Xiaona Li,[a] Jianwen Liang,[a] Matthew Zheng,[a] Yang Zhao,[a] Jiwei Wang,[a, b] Minsi Li,[a, b] Ruing Li,[a] Tsun-Kong Sham,[b] * Xueliang Sun,[a] *

[a] Department of Mechanical and Materials Engineering, University of Western Ontario, 1151 Richmond St, London, Ontario, N6A 3K7, Canada.

[b] Department of Chemistry, University of Western Ontario, London, Ontario, N6A 5B7, Canada

*Corresponding Author: Xueliang Sun, Tel: +1-519-661-2111 Ext 87759; Tsun-Kong Sham, Tel: +1-519-661-2111 Ext 86341;

E-mail address: xsun9@uwo.ca (X. Sun); tsham@uwo.ca (T.K. Sham)

# These authors contributed equally to this work.

.

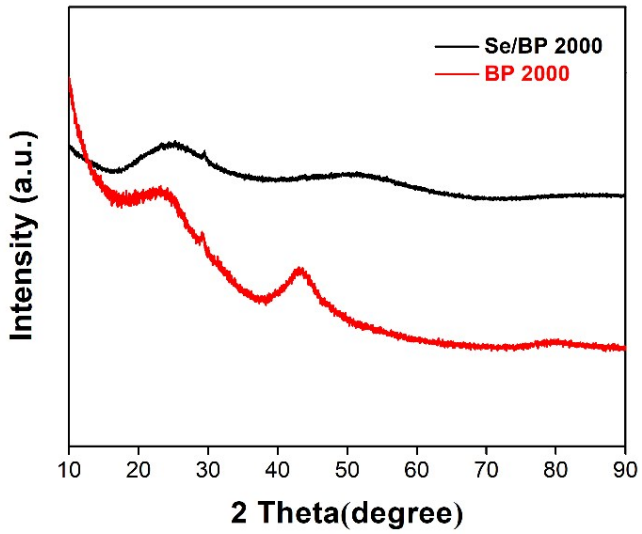

Figure S1. XRD pattern of Se/C cathode part.

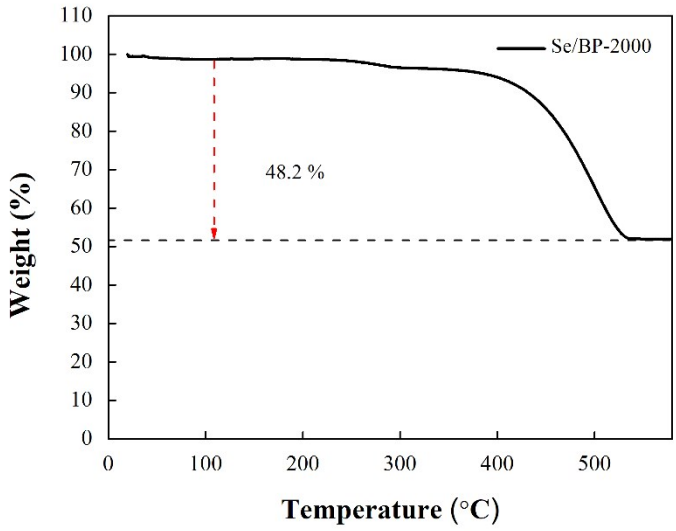

Figure S2. TGA analysis of Se/C cathode part.

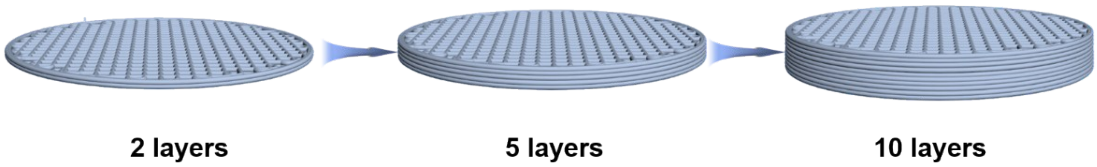

Figure S3. 3DPSe cathodes with 2 layers, 5 layers and 10 layers, corresponding with Se loading of 4 mg cm^{-2}, 10 mg $^{-2}$ and 20 mg cm^{-2}.

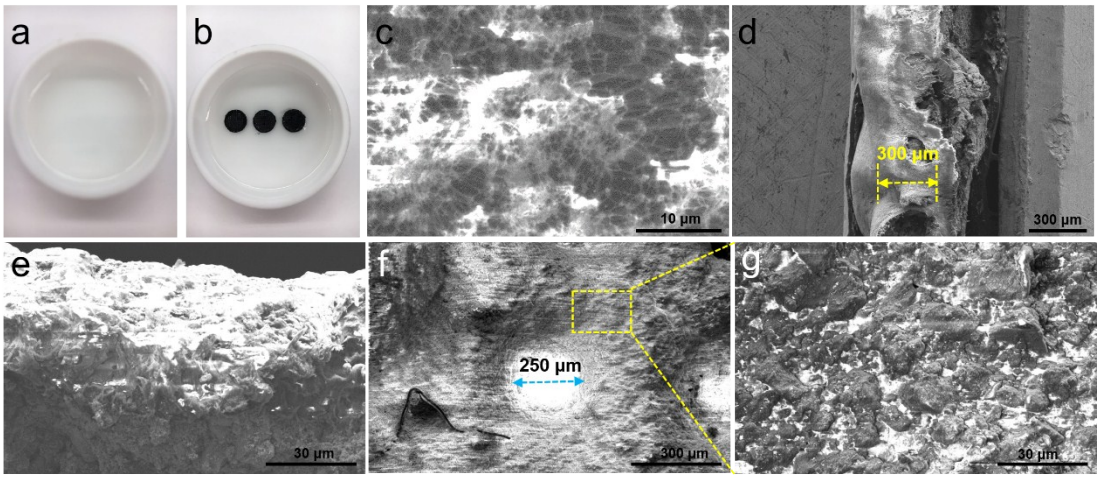

Figure S4. Morphology characterization of 3DPSe cathodes after immersing in GP. Photograph of gel-polymer (a) and 3DPSe cathodes with Se loading of 4 mg cm^{-2}, 10 mg cm^{-2} and 20 mg cm^{-2} immersed into gel-polymer (b). (c) SEM image of gel-polymer. (d, e) and (f, g): cross-sectional and top view SEM images of 3DPSe-4 cathodes after being immersed in gel-polymer at different magnification, respectively.

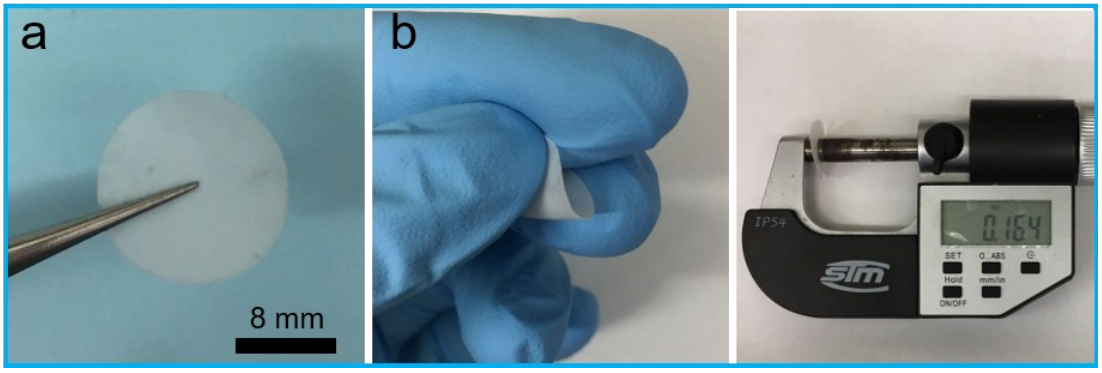

Figure S5. Photographs of gel-polymer electrolyte with a thickness of 164 µm.

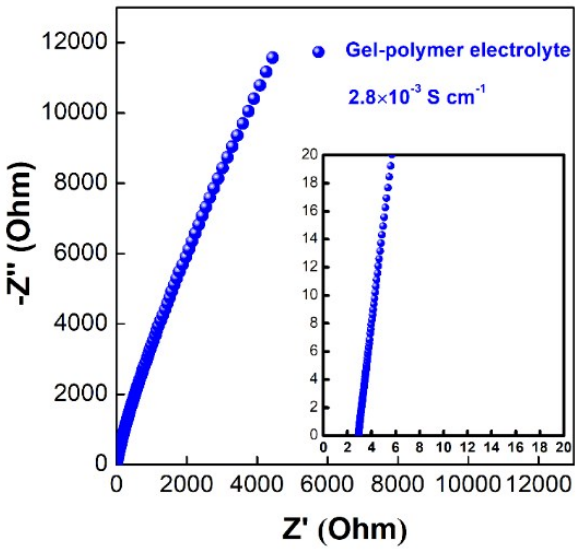

Figure S6. Nyquist plot of GPE for calculating the ionic conductivity. The insert is a magnified Nyquist plot.

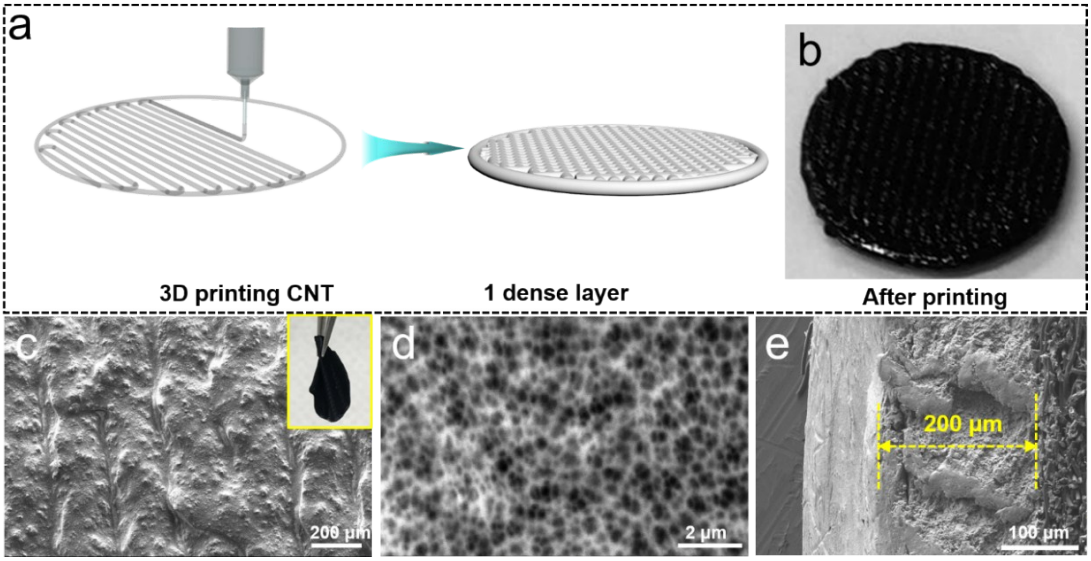

Figure S7. (a) 3D printing process of CNT and (b) digital image of printed CNT with one dense layer after printing. (c, d) SEM images of CNT under different magnifications and the inserted image shows the PCNT freestanding structure, the inset demonstrates the remarkable flexibility of the CNT interlayer. (e) Cross-sectional view.

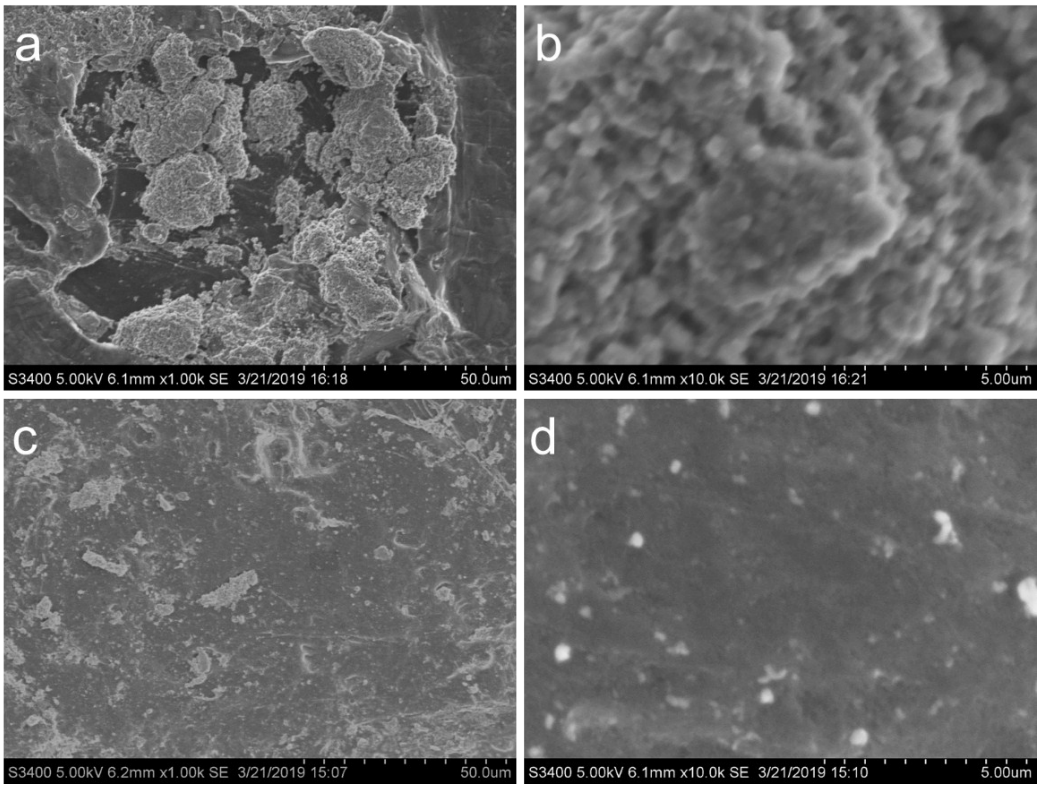

Figure S8. SEM images of Li metal anodes after 2 cycles at current density of 1 mA cm-2. (a, b) Bare Li anode. (c, d) Li/PCNT anode. The amount of Li cycled was 1.0 mA h cm^{-2}.

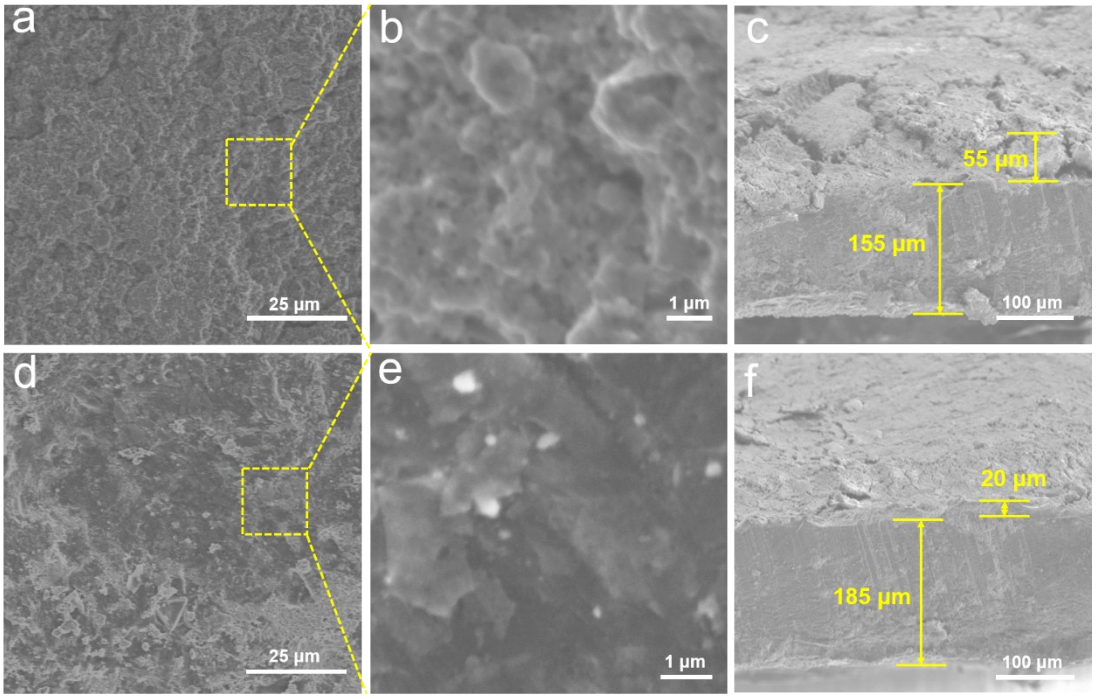

Figure S9. SEM images of Li metal anodes after 117 cycles at a current density of 1 mA cm^{-2}. (a-c) Bare Li anode. (d-f) Li/PCNT

anode. The amount of Li cycled was 1.0 mA h cm^{-2}. The inserted cross section image in (f) is Li foil before cycling.

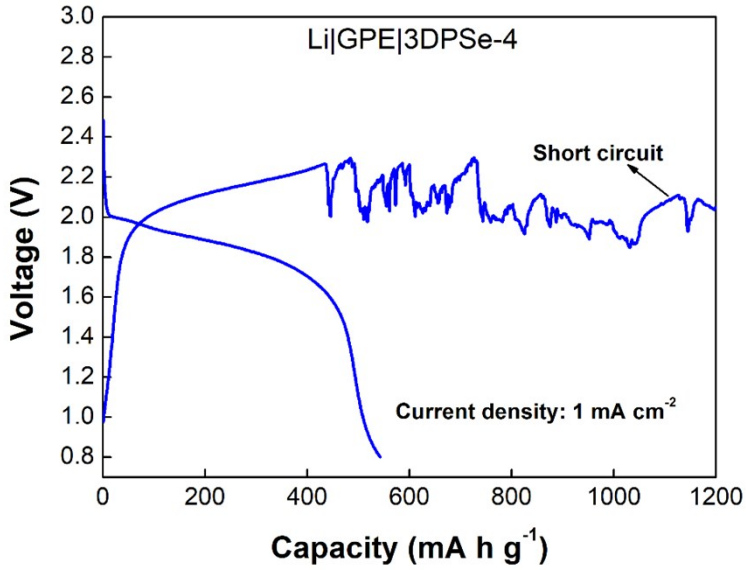

Figure S10. Charge and discharge curve of Li|GPE|3DPSe-4 at a current density of 1 mA cm^{-2}.

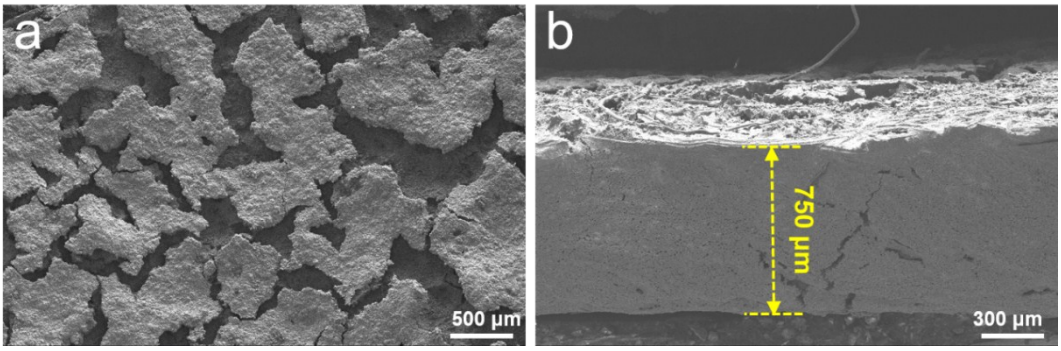

Figure S11. SEM images of BCSe-10 from top view (a) and cross-sectional view (b).

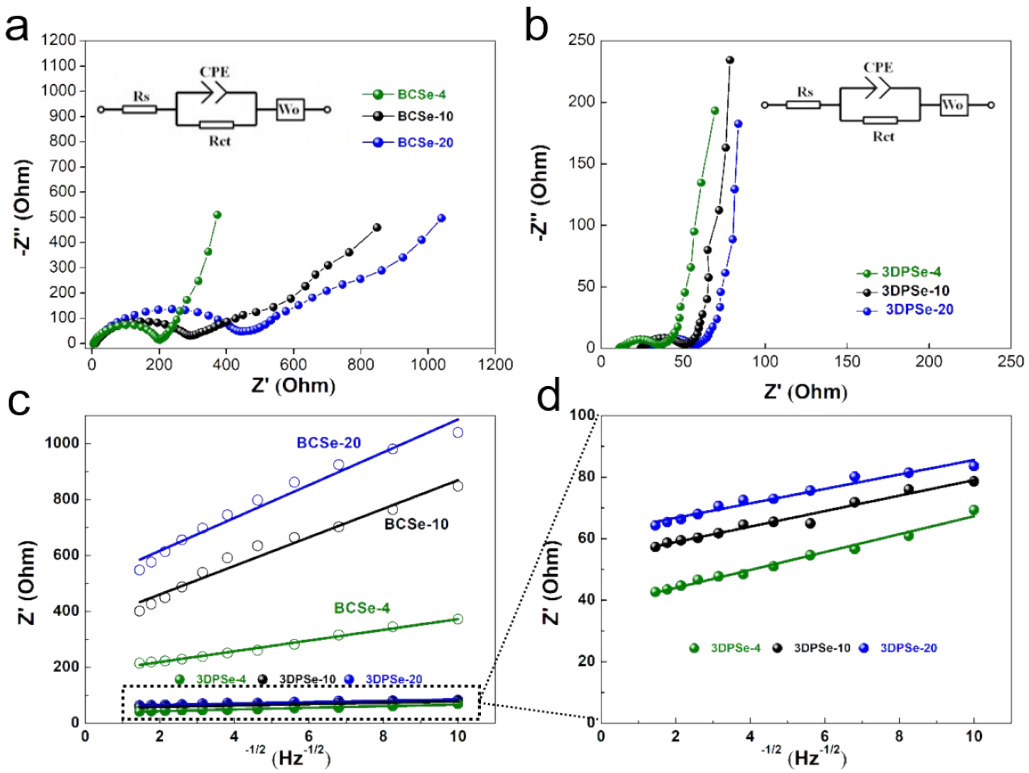

Figure S12. The electrochemical impedance spectroscopy (EIS) of BCSe-x (a) and 3DPSe-x cathodes (b) with different Se loading before cycling. (c, d) Relationship between Z' and square root of frequency ($\omega^{-1/2}$) in the low-frequency region.

Table S1. Kinetic parameters of BCSe-x cathodes and 3DPSe-x cathodes with different Se loadings.

Kinetic parameters	R_{ct} (Ω cm^{-2})	σ	D_{Li+} (cm^2 s^{-1})
3DPSe-4	29.7	2.91	4.24×10^{-10}
3DPSe-10	31.6	2.52	5.66×10^{-10}
3DPSe-20	31.3	2.35	6.51×10^{-10}
BCSe-4	199.2	19.18	9.77×10^{-12}
BCSe-10	259.2	51.06	1.38×10^{-12}
BCSe-20	400.3	58.7	1.04×10^{-12}

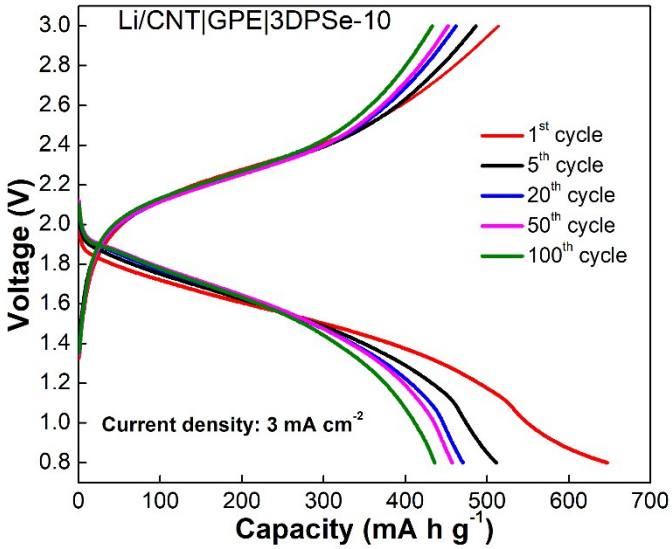

Figure S13. Charge and discharge curve of Li/CNT|GPE|3DPSe-10 at current density of 3 mA cm^{-2}.

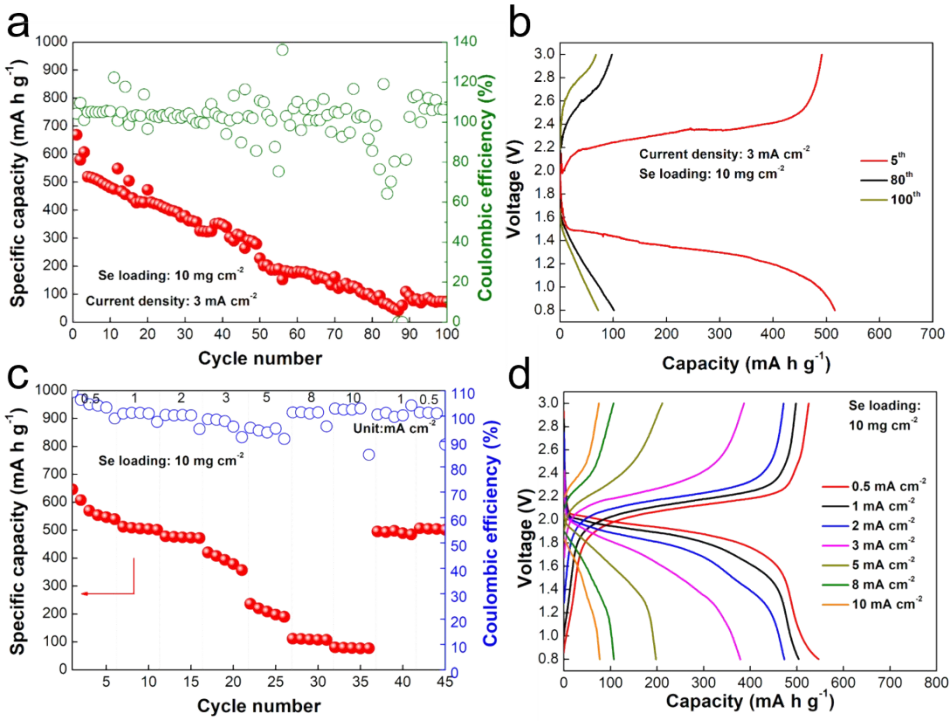

Figure S14. Electrochemical performance of Li/CNT|GPE|BCSe-10. (a) Cycling performance and (b) Charge and discharge curve at current density of 3 mA cm^{-2}. Rate performance (c) and corresponding charge and discharge curve (d) at current density from 0.5 mA cm^{-2} to 20 mA cm^{-2}.

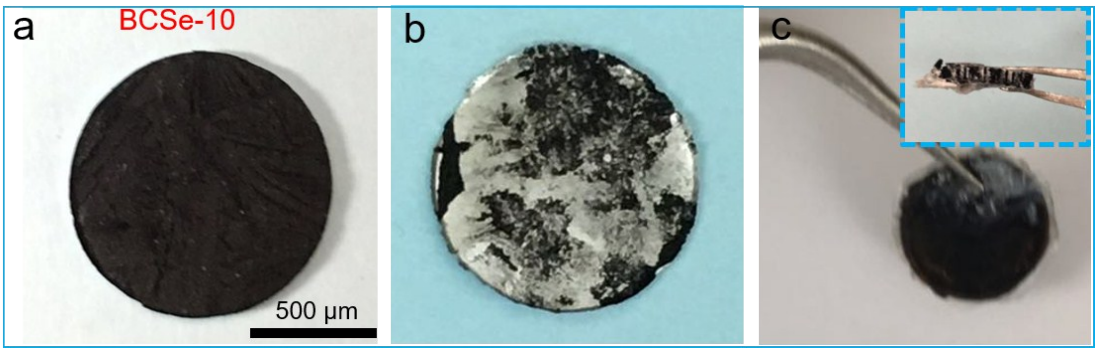

Figure S15. Optical images of BCSe-10 cathodes before (a) and after 100th cycling (b) at current densities of 1 mA cm^{-2}, 3DPSe-10 cathodes after 100th cycle (c) with the inserted image of cross-sectional optical image, still maintain a stable structure.

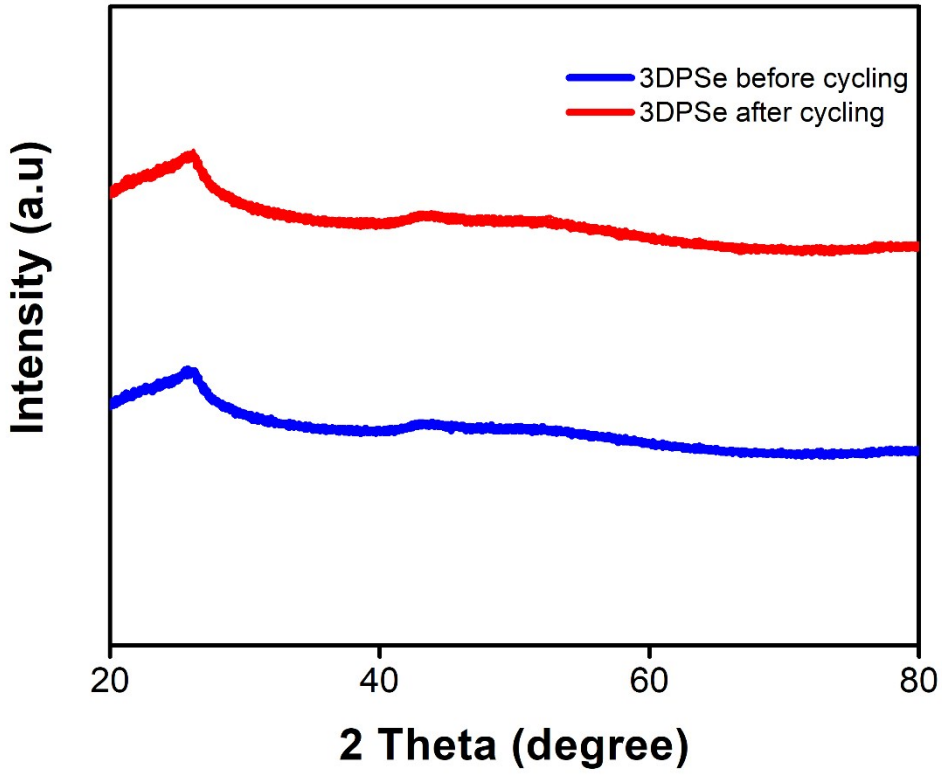

Figure S16. XRD data of 3DPSe-10 cathodes before (a) and after 100th cycling.

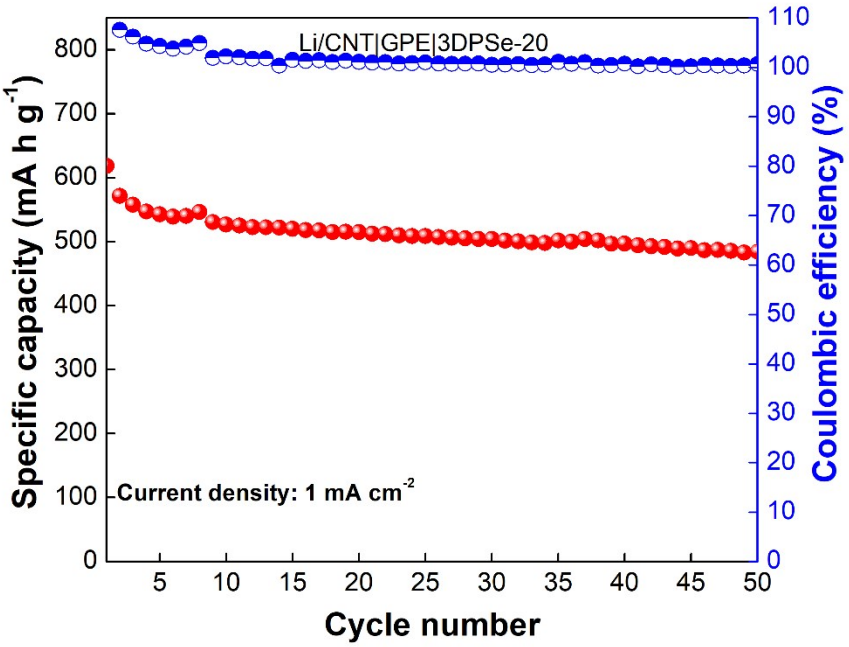

Figure S17. Cycling performance of Li/CNT|GPE|3DSe-20 at current density of 1 mA cm^{-2}.

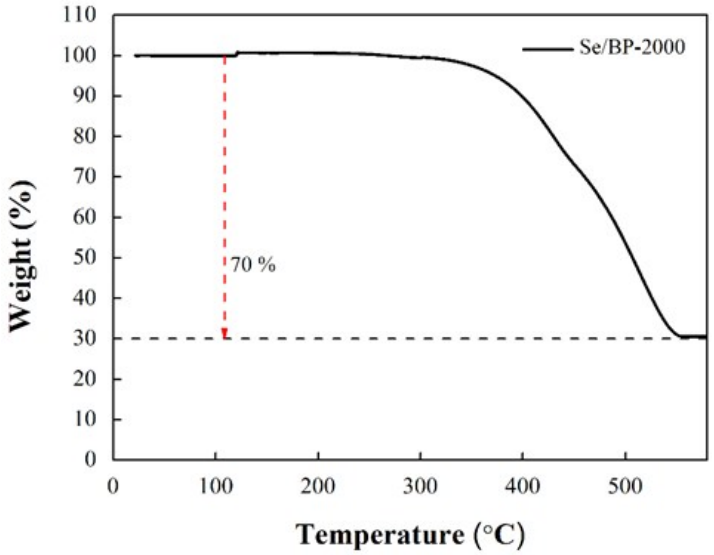

Figure S18. XRD pattern of Se/C cathode part.

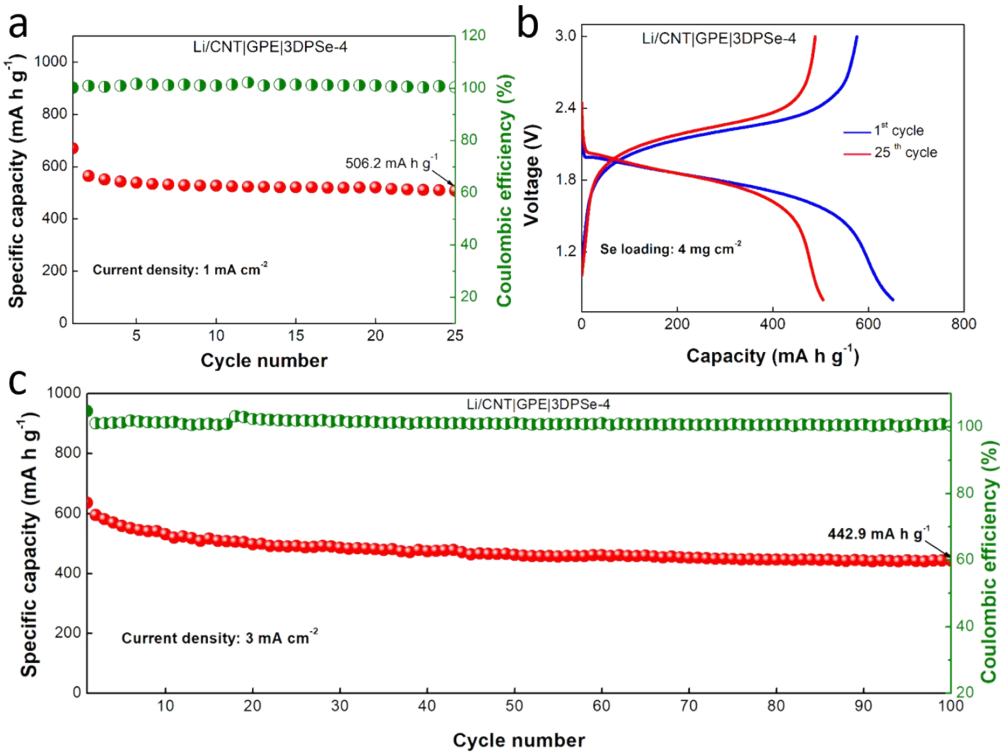

Figure S19. Cycling performance of full cell of Li/CNT|GPE|3DPSe-x (x is 4). (a, c) Cycling performance of Li/CNT|GPE|3DPSe-4 at current densities of 1 mA cm^{-2} and 3 mA cm^{-2}. (b) Galvanostatic discharge and charge curves of Li/CNT|GPE|3DPSe-4 at current density of 1 mA cm^{-2}.

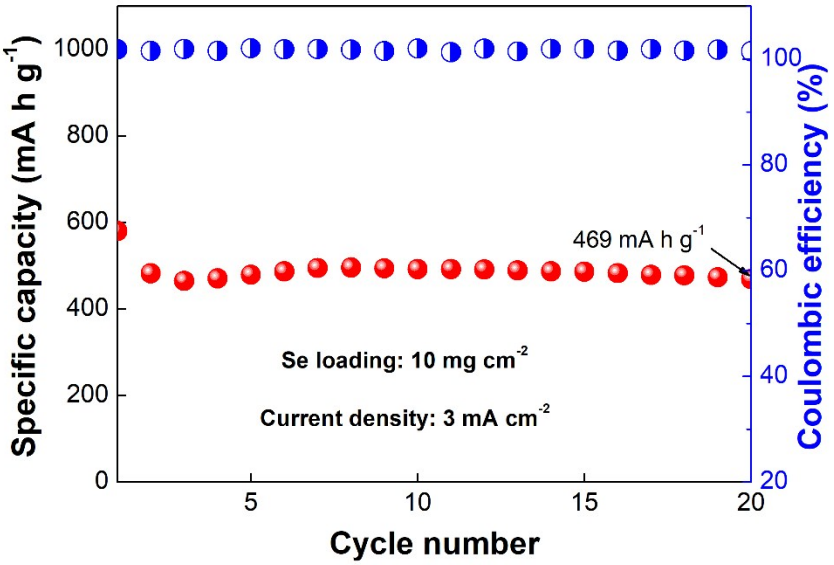

Figure S20. Cycling performance of full cell of Li/CNT|GPE|3DPSe-x (x is 10) at current densities of 3 mA cm^{-2}

Table S2. Performance comparisons with recent works at different Se loading cathodes in Li-Se batteries

Host	Se loading (mg cm^{-2})	Se content (%)	Current density (mA cm^{-2})	Specific Capacity (mAh g^{-1})	Areal capacity (mA h cm^{-2})	Year	Journal	Ref.
3DPSe-20	**20**	**48.2**	**0.5/1/2/3/5/8/10**	**640.8/539.8/508.6/477.8/414.4/321.1/266.8**	**12.82/10.8/10.2/9056/8.3/6.42/5.34**	2019	-	-
Se/MCN-RGO	1.2	62	0.41/0.81/1.62/2.43	525/462/377//274	0.63/0.55/0.45/0.33	2015	Adv. Funct. Mater.	[1]
Se@RGO	2	80	0.675/1.35/2.7/6.75	341/287/265250	0.682/0.574/0.53/0.5	2015	Journal of Power Sources	[2]
Se/CMK-3	2	49	0.675/1.35/2.7/6.75	335/238/198/152	0.67/0.48/0.396/0.3	2013	Angew. Chem. Int. Ed.	[3]
Se@flexible porous carbonnanofibers	0.8	52.3	0.27	316	0.25	2013	Adv. Energy. Mater.	[4]
Se-CDC composit	1	60	0.135/0.34/0.67/1.35	~450/420/380/350	0.45/0.42/0.38/0.35	2015	Adv. Energy. Mater.	[5]
MWCNT-Se-S	3.6	60.83	1.21/2.43/4.86/9.72	~680/580/500/358.2	2.45/2.09/1.8/1.29	2015	Journal of Power Sources	[6]

Se/N-MPCS	2	50	0.67/1.26/2.52/6.35	560/520 / 485/440	1.12/1.04/0.97/0.88	2015	J. Mater. Chem. A	[7]
Se/MMPBc	2.9±0.2	56	1/2/3	507.2/460.9/421	1.52/0.92/0.84	2015	Carbon	[8]
G@Se/PANI	3	66.18	0.41	567.1	1.7	2015	Nano energy	[9]
Se-KB	5.9	62.4	0.6	447	2.64	2017	Nano energy	[10]
Se	4	70	2.7	549	2.2	2015	ChemComm	[11]
C-Se composite	0.72	59.5	0.36	525	0.38	2017	Carbon	[12]
G–SeHMs	2–3	80	0.17/8.43	514/241	1.285/0.6	2016	Scientific report	[13]
GrapheneCNT@Se	1.6	51	0.95/3.78/9.45	558/436/192.9	0.89/0.7/0.31	2016	ACS energy letters	[14]
Se/LPC-1.0	2.4 ± 0.3	55.7	1.69/3.38/5.06/6.76	~490/430/375/350	1.23/1.08/0.94/0.88	2017	Carbon	[15]
Se/CMCs composite	1.0-1.5	~50 %	0.17/4.22	425.2/ 218.1	0.53/0.06	2017	Journal of Power Sources	[16]
Se/CNSs-850	2	60	0.67/1.35/6.75/13.5	600/550/500/390	1.2/1.1/1/0.78	2017	ACS Applied Material Interface	[17]
Se/GPNF composite	1.5 - 2	75	0.12/0.59/1.2	632/194/83	1.11/0.34/0.1	2017	ACS Energy Lett.	[18]
C-Co-N/Se	2	76.5	0.675/2.7/10.8/13.5	601.7/478.2/273.5/196.9	1.2/0.96/0.55/0.39	2017	Journal of Power Sources	[19]
HPTCs/Se composit	0.6	53	0.2/0.4/0.8	435/380/325	0.26/0.23/0.19	2017	Journal of Power Sources	[20]

e								
hollow Se@RGO	2.5	70	0.84/1.69	423/394	1.06/0.99	2017	RSC Adv.	[21]
Se-NCSs	0.8-1	56	0.3/0.61/1.22	450/320/275	0.41/0.29/0.25	2017	ACS Appl. Mater. Interfaces	[22]
NPC/CGB-Se	0.4	59.8	0.27/0.54/2.7/4.05	552/527/442/409	0.22/0.21/0.18/0.16	2018	ACS Appl. Mater. Interfaces	[23]
BP-CNF/Se	0.4	60	0.27/1.35/2.7	670/607/568	0.27/0.24/0.23	2018	J. Mater. Chem. A	[24]
Se/HDHPC	1.5	48	0.51/20	575/358	0.86/0.54	2018	Nano Energy	[25]
PANI@Se/C-G	2-3	51.9	3.4/5.06/8.4	529.2/514.2/475.6	1.3/1.29/1.19	2018	Nano Res.	[26]
Se@CoSe2-PC	1-1.2	43	0.37/0.74/3.7/7.4	509/428/275/210	0.56/0.47/0.3/0.23	2018	Electrochimica Acta	[27]
Se–NCHPC	0.7-1.0	56.2	0.57/2.87	348/261	0.3/0.2	2014	J. Mater. Chem. A	[28]
HPCA/Se	1.5-2	56	1.18/5.9	400/301	0.7/0.53	2014	Journal of Power Sources	[29]
Se/TiO2 (with carbon interlayer)	1.6	~70	0.216/0.54	282/200	0.45/0.32	2014	RSC Adv.	[30]
Se50/C	3-4	48.0	1.18/2.36	450/400	1.58/1.4	2014	Nanoscale	[31]

References:

[1] K. Han, Z. Liu, J. Shen, Y. Lin, F. Dai, H. Ye, *Advanced Functional Materials* **2015**, *25*, 455-463.
[2] X. Peng, L. Wang, X. Zhang, B. Gao, J. Fu, S. Xiao, K. Huo, P. K. Chu, *Journal of Power Sources* **2015**, *288*, 214-220.
[3] C. P. Yang, S. Xin, Y. X. Yin, H. Ye, J. Zhang, Y. G. Guo, *Angewandte Chemie International Edition* **2013**, *52*, 8363-8367.
[4] L. Zeng, W. Zeng, Y. Jiang, X. Wei, W. Li, C. Yang, Y. Zhu, Y. Yu, *Advanced Energy Materials* **2015**, *5*, 1401377.
[5] J. T. Lee, H. Kim, M. Oschatz, D.-C. Lee, F. Wu, H.-T. Lin, B. Zdyrko, W. I. Cho, S. Kaskel, G. Yushin, *Advanced Energy Materials* **2015**, *5*, 1400981.
[6] X. Wang, Z. Zhang, Y. Qu, G. Wang, Y. Lai, J. Li, *Journal of Power Sources* **2015**, *287*, 247-252.
[7] Y. Jiang, X. Ma, J. Feng, S. Xiong, *Journal of Materials Chemistry A* **2015**, *3*, 4539-4546.
[8] H. Zhang, F. Yu, W. Kang, Q. Shen, *Carbon* **2015**, *95*, 354-363.
[9] J. Zhang, Y. Xu, L. Fan, Y. Zhu, J. Liang, Y. Qian, *Nano Energy* **2015**, *13*, 592-600.
[10] Y. Zhou, Z. Li, Y.-C. Lu, *Nano Energy* **2017**, *39*, 554-561.

[11] R. Fang, G. Zhou, S. Pei, F. Li, H. M. Cheng, *Chemical communications* **2015**, *51*, 3667-3670.
[12] Y. J. Hong, Y. C. Kang, *Carbon* **2017**, *111*, 198-206.
[13] H. C. Youn, J. H. Jeong, K. C. Roh, K. B. Kim, *Scientific reports* **2016**, *6*, 30865.
[14] J. He, Y. Chen, W. Lv, K. Wen, P. Li, Z. Wang, W. Zhang, W. Qin, W. He, *ACS Energy Letters* **2016**, *1*, 16-20.
[15] H. Zhang, D. Jia, Z. Yang, F. Yu, Y. Su, D. Wang, Q. Shen, *Carbon* **2017**, *122*, 547-555.
[16] T. Liu, M. Jia, Y. Zhang, J. Han, Y. Li, S. Bao, D. Liu, J. Jiang, M. Xu, *Journal of Power Sources* **2017**, *341*, 53-59.
[17] S. F. Zhang, W. P. Wang, S. Xin, H. Ye, Y. X. Yin, Y. G. Guo, *ACS applied materials & interfaces* **2017**, *9*, 8759-8765.
[18] R. Mukkabla, S. Deshagani, P. Meduri, M. Deepa, P. Ghosal, *ACS Energy Letters* **2017**, *2*, 1288-1295.
[19] J. He, W. Lv, Y. Chen, J. Xiong, K. Wen, C. Xu, W. Zhang, Y. Li, W. Qin, W. He, *Journal of Power Sources* **2017**, *363*, 103-109.
[20] M. Jia, S. Lu, Y. Chen, T. Liu, J. Han, B. Shen, X. Wu, S.-J. Bao, J. Jiang, M. Xu, *Journal of Power Sources* **2017**, *367*, 17-23.
[21] S. Fan, Y. Zhang, S.-H. Li, T.-Y. Lan, J.-L. Xu, *RSC Advances* **2017**, *7*, 21281-21286.
[22] H. Lv, R. Chen, X. Wang, Y. Hu, Y. Wang, T. Chen, L. Ma, G. Zhu, J. Liang, Z. Tie, J. Liu, Z. Jin, *ACS applied materials & interfaces* **2017**, *9*, 25232-25238.
[23] S. K. Park, J. S. Park, Y. C. Kang, *ACS applied materials & interfaces* **2018**, *10*, 16531-16540.
[24] S.-K. Park, J.-S. Park, Y. C. Kang, *Journal of Materials Chemistry A* **2018**, *6*, 1028-1036.
[25] X. Zhao, L. Yin, T. Zhang, M. Zhang, Z. Fang, C. Wang, Y. Wei, G. Chen, D. Zhang, Z. Sun, F. Li, *Nano Energy* **2018**, *49*, 137-146.
[26] B. Wang, J. Zhang, Z. Xia, M. Fan, C. Lv, G. Tian, X. Li, *Nano Research* **2018**, *11*, 2460-2469.
[27] J. Yang, H. Gao, D. Ma, J. Zou, Z. Lin, X. Kang, S. Chen, *Electrochimica Acta* **2018**, *264*, 341-349.
[28] Y. Qu, Z. Zhang, S. Jiang, X. Wang, Y. Lai, Y. Liu, J. Li, *Journal of Materials Chemistry A* **2014**, *2*, 12255.
[29] S. Jiang, Z. Zhang, Y. Lai, Y. Qu, X. Wang, J. Li, *Journal of Power Sources* **2014**, *267*, 394-404.
[30] Z. Zhang, Z. Zhang, K. Zhang, X. Yang, Q. Li, *RSC Adv.* **2014**, *4*, 15489-15492.
[31] J. Zhang, L. Fan, Y. Zhu, Y. Xu, J. Liang, D. Wei, Y. Qian, *Nanoscale* **2014**, *6*, 12952-12957.